The Astrophysical Journal Supplement Series, 217:10 (7pp), 2015 March doi:10.1088/0067-0049/217/1/10

A LABORATORY STUDY OF C_3H^+ AND THE C_3H RADICAL IN THREE NEW VIBRATIONALLY EXCITED $^2\Sigma$ STATES USING A PIN-HOLE NOZZLE DISCHARGE SOURCE

Michael C. McCarthy[1,2], Kyle N. Crabtree[1,2,5], Marie-Aline Martin-Drumel[1,2], Oscar Martinez, Jr.[1,2,6], Brett A. McGuire[3,4], and Carl A. Gottlieb[1,2]
[1] Harvard-Smithsonian Center for Astrophysics, 60 Garden Street, Cambridge, MA 02138
[2] School of Engineering and Applied Sciences, Harvard University, Cambridge, MA 02138, USA
[3] National Radio Astronomy Observatory, Charlottesville, VA 22903, USA
[4] Division of Chemistry and Chemical Engineering, California Institute of Technology, Pasadena, CA 91125, USA
Received 2014 December 3; accepted 2015 January 28; published 2015 March 12

ABSTRACT

Rotational lines of the positive molecular ion C_3H^+ and of the neutral C_3H radical in three new vibrationally excited states with $^2\Sigma$ symmetry have been detected in a supersonic molecular beam in the centimeter-wave band. The fundamental rotational line of the ion is quite weak, but is observed with similar intensity in a dc discharge through several different hydrocarbon gases when helium is the buffer gas. Under these conditions, the fractional abundance of C_3H^+ relative to C_3H is estimated to be of order 10^{-4}, i.e., toward the lower end of the ratio (10^{-3}–10^{-4}) found for protonated ions using the same discharge nozzle. For each new $^2\Sigma$ state of the C_3H radical, spectroscopic constants, including those describing hydrogen hyperfine structure, have been determined to high precision. Lines of one $^2\Sigma$ state ($B = 11271$ MHz) are particularly intense in our molecular beam; for this state and a second one ($B = 11306$ MHz), millimeter-wave transitions have also been observed between 180 and 340 GHz using a long path dc glow absorption spectrometer. On the basis of intensity measurements with this spectrometer, the inferred rotation–vibration constant α, and theoretical calculations, the state with $B = 11271$ MHz is tentatively assigned to the ν_5 bending mode, predicted to lie $\sim$300 cm^{-1} above ground.

Key words: ISM: molecules – line: identification – methods: laboratory: molecular – techniques: spectroscopic

1. INTRODUCTION

There are a number of similarities between the radical-ion pair C_6H/C_6H^- and C_3H/C_3H^+. Both radicals possess $^2\Pi$ electronic ground states, have sizable permanent electric dipole moments (C_6H: 5.60 D, Woon & Herbst 2009; C_3H: 3.5 D, Woon 1995), and are subject to Renner–Teller (RT) interactions of the electronic and vibrational angular momenta. Rotational lines of each have been detected in the laboratory (C_6H: Pearson et al. 1988; Gottlieb et al. 2010; C_3H: Gottlieb et al. 1985; Yamamoto et al. 1990) and in space, both in their ground (C_6H: Suzuki et al. 1986; C_3H: Thaddeus et al. 1985) and in low-lying vibrationally excited states (C_6H: Cernicharo et al. 2008; C_3H: Tenenbaum et al. 2010). Electron attachment to C_6H yields an anion with a linear structure, and a highly polar, closed-shell ($^1\Sigma$) ground state (Fehér & Maier 1994), while electron detachment from C_3H, yields a cation with the same attributes (Wilson & Green 1980; Bohme et al. 1983). Although C_6H^- has now been detected in the laboratory (McCarthy et al. 2006) and in a handful of astronomical sources, mostly dark, cold molecular clouds (Gupta et al. 2009) and star-forming cores (Sakai et al. 2010; Cordiner et al. 2013), the rotational spectrum of the propynylidyne ion (l-C_3H^+) eluded measurement until quite recently.

In 2012 Pety and co-workers (Pety et al. 2012) reported rotational lines of l-C_3H^+ in the photon-dominated region (PDR) of the Horsehead Nebula. Even though rest frequencies for this ion were not available from experiment, their assignment was based on a nearly harmonic progression of transitions observed between 90 and 270 GHz that is consistent with a linear, closed-shell ($^1\Sigma$) molecule with a rotational constant $B = 11244.95$ MHz, for which l-C_3H^+ was thought to be the most likely candidate from published quantum-chemical calculations (Radom et al. 1976; Wilson & Green 1980; Ikuta 1997; Wang et al. 2007). Soon afterwards, the two lowest rotational transitions predicted from Pety et al. (2012) were also observed in absorption toward the Sgr B2(N) molecular cloud by McGuire et al. (2014a). Owing to the absence of additional rotational structure and other observational evidence (e.g., in other sources such as TMC-1, IRC+10216, etc.), these authors concluded that the astronomical lines almost certainly arise from l-C_3H^+, rather than a bent-chain isomer of C_3H^-, which had subsequently been suggested by Huang et al. (2013) and Fortenberry et al. (2013) as an alternative carrier. More recently, McGuire et al. (2014b) conducted a search for this ion in nearly 40 astronomical sources using the Caltech Submillimeter Observatory, and detected it in the Orion Bar PDR region.

Motivated by the original findings of Pety et al. (2012), laboratory searches for C_3H^+ were soon undertaken using cavity Fourier transform (FT) microwave spectroscopy of a supersonic molecular beam (McCarthy et al. 2013). We eventually found the lowest rotational transitions in a hydrocarbon discharge in exact frequency agreement with those predicted from the astronomical data, evidence that is only consistent with either linear C_3H^+ or bent-chain C_3H^-. Although our laboratory measurements cannot conclusively distinguish between positive and negative ions, the balance of evidence seemed to favor the cation. In an elegant experiment by Brünken et al. (2014) using a cryogenic ion trap apparatus, and a novel mass-selective action spectroscopy based on light-

[5] Present address: Department of Chemistry, University of California-Davis, Davis, CA 95616, USA.
[6] Present address: Air Force Research Laboratory, Space Vehicles Directorate, 3550 Aberdeen Avenue SE, Kirtland AFB, NM 87117-5776, USA.

induced reactions, the carrier was unambiguously shown to arise from l-C_3H^+.

Detection of C_3H^+ in space is intriguing because it is known to react with H_2 (Anicich & Huntress 1986; Savić & Gerlich 1994), and for a very long time there was only one astronomical molecular ion that reacts similarly:[7] CH^+. Additionally, chemical models (Turner et al. 2000; Wakelam et al. 2010) predict that this cation is a central intermediate in the gas-phase synthesis of small hydrocarbons such as C_3H and C_3H_2. However, the column densities of these species are much greater in PDRs than predicted from these models alone, a finding which suggests that other formation pathways may be operative. Because C_3H^+ is plausibly formed from C_3H in our discharge molecular beam, the experimental conditions that were used to detect this cation, such as the choice of precursor and carrier gases, as well as the fractional abundance of the cation relative to the neutral radical, might serve as a guide by which related cations can be produced and detected by similar means. With accurate laboratory rest frequencies, radioastronomical searches would then be undertaken with confidence, thereby constraining the formation pathways in astronomical sources where small hydrocarbons are abundantly found.

In the course of this investigation, three new vibrationally excited states of C_3H radical with $^2\Sigma$ symmetry were detected, in addition to the previously reported $v_4 = 1$ $^2\Sigma^\mu$ state, which was first observed in the laboratory by Yamamoto et al. (1990). Owing to a large RT interaction between the $^2\Sigma^\mu$ state in the CCH bending mode ν_4 ($\sim$600 cm^{-1} above ground) and the $^2\Pi_{3/2}$ spin component in the ground vibrational state, the $^2\Sigma^\mu$ state is shifted to within 20 cm^{-1} of the $^2\Pi$ ground state. The spectroscopic constants of the $^2\Sigma^\mu$ state were subsequently refined following new measurements in the submillimeter band that included direct rovibrational transitions between the $^2\Sigma^\mu$ and $^2\Pi_{3/2}$ states (Caris et al. 2009).

One new $^2\Sigma$ state with $B = 11271$ MHz (hereafter designated simply by its rotational constant, i.e., $B11271$) is particularly intense in our gas expansion; the intensity of its lines is largely insensitive to the choice of the carrier gas (e.g., He versus Ne), and they are more than 40 times more intense than those of the other three Σ states. Using a long path dc glow discharge absorption spectrometer, its spectrum, along with that of a second state with $B = 11306$ MHz (B11306), has now been measured well into the millimeter-wave band (up to 340 GHz) and its line intensities compared to those from the ground state. From the inferred rotation–vibration constant α, theoretical calculations, and on the assumption that the vibrational temperature is similar to that of C_4H (Cooksy et al. 2015), we tentatively assign $B11271$ to the ν_5 bending vibrational mode, lying roughly 450 K above ground.

2. EXPERIMENTAL DETAILS

The majority of the experiments described here were undertaken with a sensitive cavity FT microwave spectrometer, which has been previously used to detect the rotational spectra of a variety of molecular ions and other short-lived intermediates (McCarthy et al. 2000), including both molecular anions (Lattanzi et al. 2010) and protonated species (Gottlieb et al. 2000). It operates from 5 to 42 GHz, but higher-frequency transitions can often be detected using double resonance (DR) spectroscopy (Jäger & Gerry 1995; Sumiyoshi et al. 2005). In this type of experiment (Crabtree et al. 2013), the intensity of a line that falls in the operating band of the cavity spectrometer is monitored as a second radiation source is swept in frequency. Normally, this second source propagates perpendicular to the axis of the Fabry-Perot cavity, typically near the beam waist. A pronounced decrease in the intensity of this line normally occurs when the frequency of the tunable radiation source exactly coincides with another rotational transition of the same molecule, and the two transitions share either an upper or lower state.

Although the fundamental transition of C_3H^+ lies near 22.5 GHz, well within the frequency range of the FT microwave spectrometer, the $J = 2$–1 transition lies just beyond the frequency range, and could only be detected by DR spectroscopy. The same situation applies to the new vibrationally excited states of C_3H, in which DR was used to confirm that the observed lines arise from a molecule in a $^2\Sigma$ state with a rotational constant within $\pm 1\%$ of that of the ground state.

The intensity of the 1–0 line of C_3H^+, although faint, was not sharply optimized with any experimental parameter; typical conditions were 0.05% acetylene (C_2H_2) in He, and a discharge potential of 1 kV. At a repetition rate of 6 Hz of the nozzle, a backing pressure of 2.5 kTorr, and a gas pulse duration of 480 μs, the gas flow rate was about 60 cm^3/minute at standard temperature and pressure. Lines of comparable intensity were also observed with diacetylene (HC_4H) or methylacetylene (CH_3CCH) at roughly the same level of dilution. Transitions of new vibrationally excited states of C_3H were observed under similar experimental conditions to those of C_3H^+, except that their intensity did not sensitively depend on the carrier gas, with Ar and Ne giving somewhat stronger lines compared to He.

Once the two lowest rotational transitions of vibrationally excited C_3H were detected and assigned, attempts were then made to extend these measurements to the millimeter band using long-path absorption spectroscopy and a low-pressure glow discharge (Gottlieb et al. 2010). In this spectrometer, C_3H was produced in high concentration using a gas mixture of C_2H_2/Ar/He/CO in the molar ratio 10:1:5:10, a discharge current of 200 mA, and a voltage of 1 kV. With the walls cooled to 170 K using liquid nitrogen, the base pressure in the cell was approximately 25 mTorr. To improve the signal-to-noise ratio, tunable millimeter radiation passes twice through the absorption cell: it first passes through a grid polarizer and then propagates along the length of the discharge, where it then is reflected by a roof-top mirror, rotating the plane of polarization by 90°. After counter-propagating back through the cell, radiation is reflected by the grid polarizer where it is detected by a sensitive, liquid He cooled InSb detector. Line profiles were fit using the second-derivative of a Lorentzian, a line shape resulting from the convolution of pressure broadening, and the frequency modulation and detection scheme ($2f$) used to suppress $1/f$ noise. Measurements of relative intensities were made by systematically comparing line intensities for the same rotational transition ($N = 12$–11) of various vibrationally excited states to that of the $^2\Pi_{1/2}$ ground state near 270 GHz.

[7] During the past few years, a number of small ions that also react with H_2 have been detected in space using the *Herschel* Space Observatory. These ions include OH^+, H_2O^+, SH^+, HCl^+, ArH^+, among others (Schilke et al. 2014, and references therein).

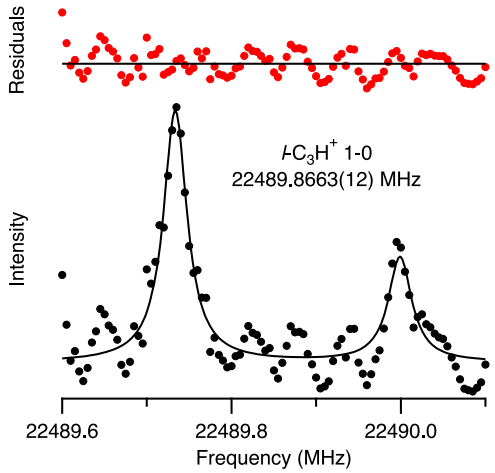

Figure 1. The spectrum of the fundamental transition of l-C_3H^+ at 22489.8663 ± 0.0012 MHz after ~7.5 hr of integration, although the line is initially detectable with lower signal-to-noise ratio in as little as 15 minutes of integration. The Doppler splitting arises because the supersonic molecular beam propagates coaxially with the axis of the Fabry–Perot resonator. The frequency was determined from a fit to a pair of Doppler-split Lorentzian profiles with a common rest frequency.

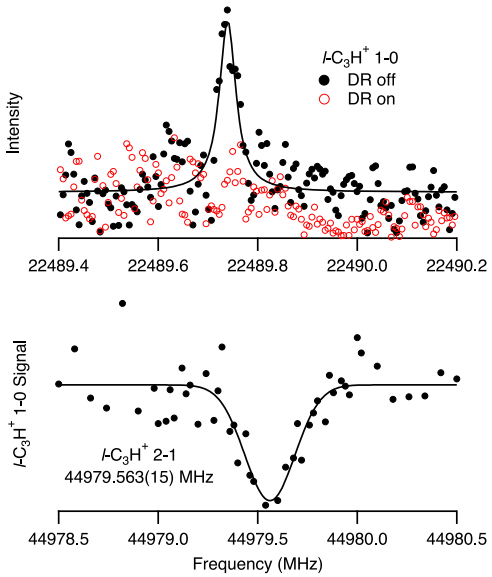

Figure 2. (Top) FT microwave spectrum of the redshifted Doppler component of the 1–0 transition of l-C_3H^+ with (red open circles) and without (black filled circles) DR radiation at 44979.540 MHz. (Bottom) DR spectrum of the 2–1 transition of l-C_3H^+, acquired after a total of about 10 hr integration. The center frequency is derived from a fit to a Gaussian profile.

3. RESULTS

3.1. C_3H^+

Because the uncertainty in the rest frequency of the fundamental transition of C_3H^+ (22489.865 ± 0.002 MHz) from the astronomical data of Pety et al. (2012) alone is very small compared to the instantaneous bandwidth of our FT microwave spectrometer (~0.5 MHz), reproducing the same line in the laboratory only requires experimentation with different precursor gases and optimization of the source chemistry. To produce C_3H^+, a gas mixture of C_2H_2 heavily diluted in Ne (0.1%) was initially used, negative high voltage was applied to the copper electrode farthest from the nozzle (a discharge polarity previously found to favor production of protonated species), and the chemistry was optimized to produce the C_3H radical in high abundance, by analogy to the radical-ion pair C_6H/C_6H^- where production of the two species appears to be correlated (McCarthy et al. 2006). However no line was found after very long integrations, and even when the acetylene concentration was varied by roughly an order of magnitude (from 0.02 to 0.25%). Replacing Ne with H_2 proved equally futile, even though this carrier gas has been used with good success to detect nearly a dozen protonated molecules (Gottlieb et al. 2000) and several molecular anions (McCarthy & Thaddeus 2008). When He was used instead, however, a weak feature with no apparent line structure was soon observed (Figure 1). Its frequency (22489.8663 ± 0.0012 MHz) is within 2 kHz of that predicted, either from the 2-parameter fit of Pety et al. (2012) or the laboratory measurements of Brünken et al. (2014), making the probability of a chance coincidence from an unrelated molecule highly unlikely from this measurement alone.

Follow-up tests and measurements quickly established that the newly detected line arises from C_3H^+, and no other molecule. The line is only observed in a hydrocarbon discharge, and its intensity decreases when a permanent magnet is placed near the molecular beam, consistent with the behavior expected for an ion with a closed-shell electronic state: the Lorentz force on a charged molecule in the collisionless environment of a supersonic beam induces collisional dephasing of the molecular free induction decay. If the carrier were instead open-shell, the magnetic field would produce detectable Zeeman splittings in the spectrum, while the intensities and linewidths of a neutral closed-shell molecule would be unaffected.

Ultimately, DR spectroscopy was undertaken to remove any remaining ambiguity as to the identity of the carrier. Shown in Figure 2 (bottom) is the spectrum recorded when tuning the frequency of the DR source across the predicted 2–1 line of C_3H^+, while integrating the line intensity of the corresponding 1–0 transition at each step. Owing to the low signal-to-noise ratio, many minutes of integration were required at each step, but even at this level, a decrease in the line intensity is evident at the on-resonance condition (Figure 2, top). The frequency derived by this procedure (44979.563 ± 0.015 MHz) and that reported by Brünken et al. (2014; 44979.536 ± 0.014 MHz) differ by only 0.027 MHz, which is comparable to the combined 1σ uncertainty of the two measurements.

A fit of our laboratory measurements to effective Hamiltonian for a linear molecule yields constants of $B_{\rm eff} = 11244.9473 \pm 0.0015$ MHz and $D_{\rm eff} = 7.07 \pm 0.63$ kHz, where the uncertainties reflect the 1σ uncertainties in the experimentally determined frequencies. Not surprisingly, these values almost exactly match the constants derived from the astronomical measurements (Pety et al. 2012, $B_{\rm eff} = 11244.9474 \pm 0.0007$ MHz; $D_{\rm eff} = 7.652 \pm 0.011$ kHz), and Brünken et al. (2014). On the assumption that the dipole moment is 3D, we estimate that of order 5×10^8 C_3H^+ ions are produced per gas pulse, by calibrating with a stable molecule of known concentration (0.2% OCS in Ar), and correcting for differences in the rotational partition functions and dipole moments.

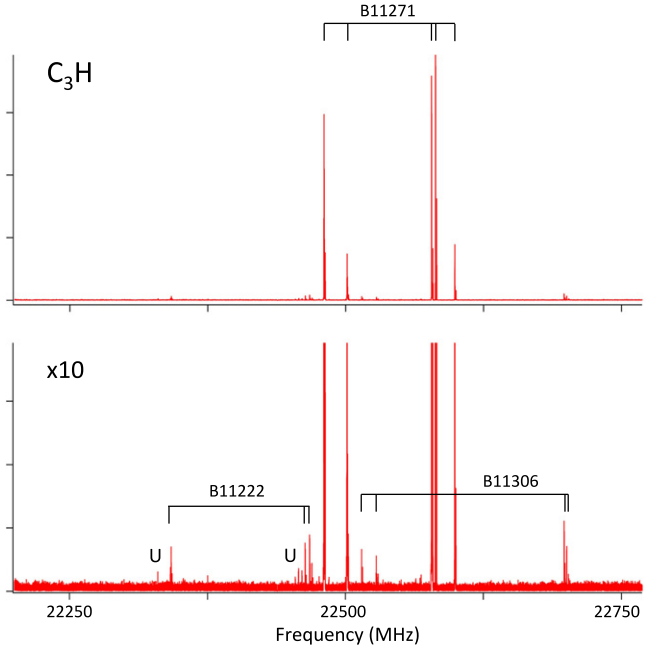

Figure 3. FT microwave spectrum near 22.5 GHz, showing the fundamental rotational lines of several $^2\Sigma$ states of C_3H observed in a supersonic beam. (Top) The spectrum plotted full-scale, and (bottom) when the vertical axis is magnified by a factor of 10. The survey, recorded by applying an electrical discharge to a dilute gas mixture of acetylene (0.1%) in Ne, is a concatenation of 1425 individual scans, each spanning 0.4 MHz, and is the result of 13.5 hr of integration. Lines marked with a "U" are unidentified, but likely arise from still other $^2\Sigma$ states of the same radical. As indicated in Figure 1, each line possesses a double-peaked line shape owing to the Doppler effect.

3.2. Vibrationally Excited C_3H

Frequency surveys covering about ±1% around the 1–0 line of C_3H^+ were performed, to determine if more intense lines exhibiting the same behavior under our experimental conditions lie nearby. To our surprise, a number of features, some very intense, were detected (Figure 3). Assays establish that these lines, in contrast to that of C_3H^+, broaden or split into multiple components even when a small external magnetic field is applied, implying that the carrier is paramagnetic. None of the lines shown in Figure 3 arise from the low-lying $v_4 = 1\ ^2\Sigma^\mu$ state, but weak lines from this state were observed (Table 1) after deep integrations at frequencies predicted from the higher-frequency laboratory data of Yamamoto et al. (1990).

In contrast to C_3H^+, the unidentified lines are also observed with comparable or greater intensity in a Ne expansion, implying that their production is closely correlated in an absolute sense with that of C_3H. Although the assignment of most features is not readily apparent, an indication of the quantum number F and how F changes with the pattern-forming quantum number J was possible by examining the characteristic Zeeman pattern of a line in the presence of a small magnetic field; transitions with $\Delta F = -1$, for example, behave quite differently than those with $\Delta F = 0$ or +1. Once tentative assignments were made, DR spectroscopy was used to link lines sharing a common upper or lower state, and to extend the measurements to higher frequency. In total, at least 12 hyperfine-split transitions were observed for each new vibrationally excited state (Table 1).

Higher-frequency lines have now been found in the millimeter band for two of the three new $^2\Sigma$ states. Lines were generally detected within ± 10 MHz of the frequencies extrapolated from the low-frequency data, and at least four spin-rotation doublets were measured between 180 and 340 GHz (Table 2). As the sample spectra in Figure 4 illustrate, lines from both states were observed with good signal-to-noise ratio in only a few minutes of integration (i.e., at least 10 after 10 minutes).

In addition to precise frequencies, the millimeter-wave measurements also provide fairly accurate relative intensities of rotational satellites (typically to ±15%). For the closely related CCH (Killian et al. 2007) and C_4H radicals (Cooksy et al. 2015), this intensity information has been used with good success to make assignments to specific vibrational states because the vibrational temperature of bending modes has been shown to be closely coupled to the wall temperature of the cell. Such an empirical correlation between intensity and energy is possible for these two radicals because accurate energies for a number of low-lying vibrational states (up to ~800 K) have been predicted from theory (CCH: Sharp-Williams et al. 2011, and references therein; C_4H: Graf et al. 2001) and derived from optical (C_4H: Mazzotti et al. 2011) or infrared measurements.

Using an isolated $^2\Sigma$ Hamiltonian, four spectroscopic constants were required to reproduce the centimeter-wave rotational spectrum of each new vibrationally excited state of C_3H: the rotational constant B, the spin-rotation constant γ, and two terms (b_F and c) describing the hydrogen hyperfine structure. When the millimeter-wave measurements are added to the data set, two additional distortion terms (D and γ_D) are needed. The derived spectroscopic constants are summarized in Table 3, along with those for the low-lying $v_4 = 1\ ^2\Sigma^\mu$ state, which now include the new 1–0 measurements. Because the frequencies for the hyperfine-split lines in the fundamental rotational transition of this state were uncertain to 20–150 kHz prior to this work, the measurements here reduce these uncertainties by roughly an order of magnitude, and thereby improve the accuracy of the two hydrogen hyperfine constants by a similar amount.

4. DISCUSSION

4.1. C_3H^+

Although the line intensity of C_3H is 3–5 times weaker in He compared to Ne, C_3H^+ is only detected using this carrier gas. Use of He (as opposed to Ar or H_2) was also essential for the detection of the chemically similar CH^+ ion by Amano (2010), even though this experiment was performed in a long-path discharge cell, rather than the pin-hole discharge nozzle source employed here. Although the role that He plays in our discharge source is uncertain, it results in a faster molecular beam, which decreases the total number of electron recombination reactions on the timescale of expansion. Like H_2, it may generally favor formation of molecular ions (Gottlieb et al. 2000; McCarthy & Thaddeus 2008).

By comparing line intensities of C_3H^+ and C_3H, and correcting for differences in the partition functions (the dipole moments are comparable), we estimate a C_3H^+/C_3H fractional abundance in the range 0.5×10^{-5}–1×10^{-4}, irrespective of the hydrocarbon precursor. Although we cannot be certain that C_3H^+ is formed via electron detachment from C_3H, all three precursors (C_2H_2, HC_4H, and CH_3CCH) abundantly produce this radical, and its chemistry was optimized prior to detection of C_3H^+. As a cautionary note, in space this ion is instead

Table 1
Centimeter-wave Rotational Frequencies of C_3H in Four $^2\Sigma$ Vibrationally Excited States

Transition			$v_4 = 1$	$B11222$	$B11271$	$B11306$
$N' \rightarrow N''$	$J' \rightarrow J''$	$F' \rightarrow F''$	$^2\Sigma^\mu$			
1 → 0	1/2 → 1/2	1 → 0	22472.0534	22373.0424	22484.2293	22522.2501
		0 → 1	⋯	22373.6601	22484.3919	22511.7028
		1 → 1	⋯	22390.2150	22501.0587	22523.6225
	3/2 → 1/2	1 → 0	22422.5483	22470.7862	22562.3405	22660.2793
		2 → 1	22419.8175	22473.8804	22565.1989	22658.4300
		1 → 1	22421.5019	22487.9567	22579.1700	22661.6679
2 → 1	3/2 → 3/2	1 → 1	…	44746.533	44968.459	45033.8036
		2 → 1	…	⋯	44981.792	⋯
		1 → 2	…	⋯	44982.436	⋯
		2 → 2	…	44773.970	44995.772	45044.433
	3/2 → 1/2	1 → 1	…	⋯	45046.582	45171.849
		2 → 1	…	44857.615	45059.906	45179.249
		1 → 0	…	⋯	45063.231	45183.688
	5/2 → 3/2	2 → 1	…	44917.479	45106.662	45272.281
		3 → 2	…	44918.097	45107.274	45271.740
		2 → 2	…	44931.566	45120.642	45275.555

Note. Units are MHz. The 1σ uncertainties are 5 kHz for measurements below 25 GHz, and 10–25 kHz above this frequency.

Table 2
Millimeter-wave Transitions of the $B11271$ and $B11306$ ($^2\Sigma$) States of C_3H

	$J = N - \frac{1}{2}$		$J = N + \frac{1}{2}$	
$N' \leftarrow N''$	Frequency	Obs.-Calc.	Frequency	Obs.-Calc.
		$B11271$		
8 ← 7	180297.345	−0.010	180346.409	0.003
9 ← 8	202833.926	0.006	202883.139	−0.005
10 ← 9	225369.217	0.003	225418.627	0.025
11 ← 10	247903.087	−0.008	247952.650	−0.008
12 ← 11	270435.416	−0.002	270485.154	−0.018
14 ← 13	315394.844	−0.001	315545.007	−0.003
15 ← 14	338021.669	0.009	338072.054	0.001
		$B11306$		
8 ← 7	180843.260	−0.023	180936.752	−0.021
9 ← 8	⋯	⋯	203543.971	−0.022
10 ← 9	226055.684	−0.070	226149.745	−0.014
11 ← 10	248659.591	−0.016	248753.878	−0.032
12 ← 11	271261.662	0.005	271356.298	0.016

Note. Units are MHz. Measurement uncertainties are in the range of 15–30 kHz. Calculated frequencies are derived from the best-fit constants in Table 3.

thought to be formed from the reaction between C^+ and HCCH (Lindemann et al. 1972), a formation route that cannot be ruled out in our experiment. The derived ratio is somewhat lower than that found for protonated molecules (10^{-3}–10^{-4}; Gottlieb et al. 2000) using the same nozzle source. More generally, this result may suggest that positive ions of abundant molecules might be present at a fairly constant level compared to their neutral counterpart.

Other small cations might conceivably be detected by similar means. Like negatively charged ions, the most promising candidates are abundantly produced radicals for which electronic detachment yields a highly polar cation with a closed-shell electronic ground state. For these reasons, C_5H^+ and propargyl cation (H_2CCCH^+) appear to be particularly attractive targets. C_5H is abundantly produced using the same nozzle source (McCarthy & Thaddeus 2005), and calculations (Botschwina 1991; S. Thorwirth 2013, personal communication) conclude that C_5H^+ is both highly polar ($\mu = 2.88$ D) and possesses the desired $^1\Sigma$ ground state. Intense lines of H_2CCCH have also been detected by FT microwave spectroscopy (Tanaka et al. 1997) in a molecular beam, even though this radical has a very small dipole moment (~0.1 D) and the intensity of each rotational line is diluted over many individual fine and hyperfine components. In contrast, the H_2CCCH^+ ion is predicted to possess a modest dipole moment (0.5 D), and removal of an electron to form the positive ion results in a closed-shell ground state (Botschwina et al. 2011) whose partition function is quite small—factors that should greatly aid detection in the laboratory and in space.

4.2. Vibrationally Excited C_3H

C_3H has a complex vibronic structure which, owing to RT effects, is so pronounced in the ground electronic state that the $v_4 = 1$ $^2\Sigma^\mu$ state is shifted to within 30 K of the $^2\Pi_{1/2}$ ground state. The most sophisticated theoretical treatment to date by Perić et al. (2003) predicts the ν_4 vibration has a large RT coupling constant ($\epsilon = -0.883$), but this constant is smaller by nearly a factor of three for ν_5 ($\epsilon = +0.333$). When both vibronic and spin–orbit couplings are computed using a variational approach, the predicted low-lying vibrational energy structure, including both spin–orbit splitting and the small energy difference between the ground and first excited vibronic mode, is in good agreement with experiment. These calculations also predict that the two $^2\Sigma$ states of $v_5 = 1$ lie approximately 360 and 510 K above ground, while the $v_4 = 1$ $^2\Sigma^\kappa$ state is shifted above 1000 K. Because vibrational frequencies have only been measured in Ar matrices for ν_1, ν_2, and ν_3 (Jiang et al. 1993), however, and no rotationally resolved spectra from low-lying vibronic states have been reported from optical (Ding et al. 2001) or infrared studies, vibrational assignments for the newly detected $^2\Sigma$ states must be regarded as tentative.

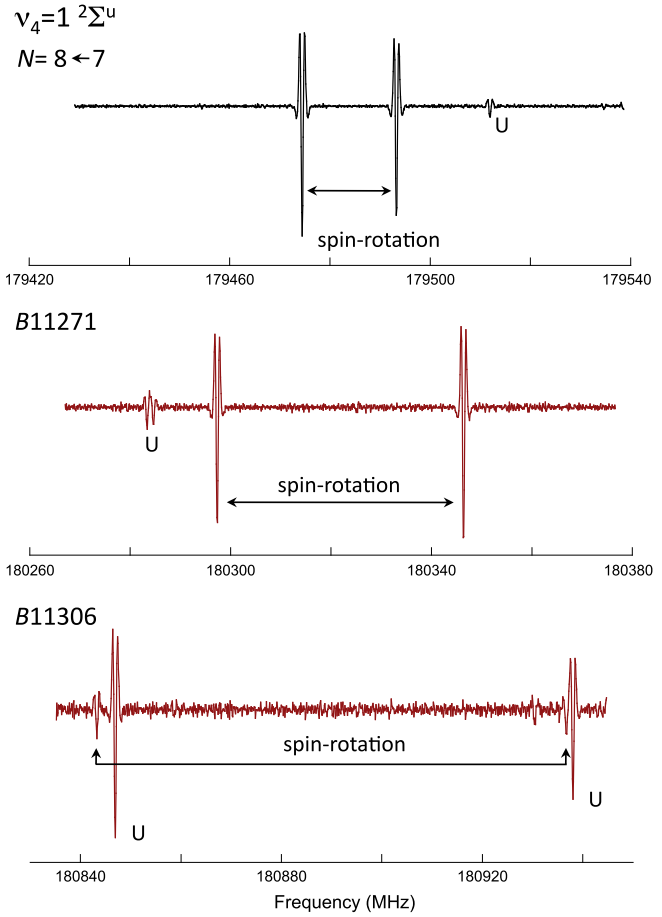

Figure 4. Sample rotational spectra for the $N = 8 \leftarrow 7$ transition of several vibrationally excited $^2\Sigma$ states of C_3H radical near 180 GHz. The spin-rotation doublet is indicated for each transition; lines marked with a "U" are unidentified. The integration time was 22 minutes for each spectrum. The second derivative line shape is a result of the frequency modulation (f) and detection ($2f$) scheme employed to reduce $1/f$ noise.

From the relative intensity measurements in Section 2, estimates or lower-limits for the energies of the new $^2\Sigma$ states have been made (Figure 5), on the assumption that each arises from a low-lying bending mode, and that the vibrational temperature is the same as that derived from C_4H (Cooksy et al. 2015). The former assumption appears quite solid because the rotational–vibrational constants α_i are uniformly negative, as expected for bending modes, which normally decrease the moment of inertia, and thereby yield larger rotational constants compared to the ground state. From Figure 5, we conclude $B11271$ lies about 450 K above ground, which implies it originates from one of the two $^2\Sigma$ states of the ν_5 bend, in part because no other vibrational state is predicted within 500 K of this value. Although anecdotal, this energy is also consistent with previous FT microwave experiments which studied vibrational excitation in electrical discharge nozzles. These studies (Sanz et al. 2005) found that strong rotational satellites frequently originate from vibrational states lying near kT (of order 300–600 K), presumably because the collisional frequency is insufficient to quench states of this energy on the timescale of the expansion. Given the much higher energy inferred from the same plot, the assignment of $B11306$ to a specific mode or combination band cannot be made with confidence.

Table 3
Spectroscopic Constants of C_3H in Four Excited Vibrational Levels with $^2\Sigma$ Symmetry

Constant[a]	$v_4 = 1$ $^2\Sigma^\mu$	$B11222$	$B11271$	$B11306$
B	11212.783(21)	11221.9298(10)	11270.8692(3)	11306.4964(10)
10^3D	5.0084(17)	5.01[b]	5.8669(11)	6.788(4)
γ	−35.400(13)	61.7683(26)	48.6896(14)	92.644(3)
$10^3\gamma_D$	1.44(16)	1.44[b]	2.571(16)	4.63(4)
b_F	1.038(6)	−17.170(5)	−16.833(4)	−1.381(5)
c	28.35(4)	25.23(13)	25.880(10)	25.823(13)
σ (MHz)	0.028	0.018	0.007	0.026
χ^2_{red} [c]	1.57	0.84	0.78	0.98
α (MHz)[d]	−23.7	−32.9	−81.8	−117.4
ΔE (K)[e]	28	>1600	~450	~1500

Note. Units are MHz, unless otherwise noted. The 1σ uncertainties (in parentheses) are in units of the last significant digit.
[a] Derived from a least-squares fit to the measurements in Table 1 alone, or in combination with those in Table 2 and those from Yamamoto et al. (1990).
[b] Constrained to the value derived for the $^2\Sigma^\mu$ state.
[c] The reduced χ^2 error, $\chi^2_{red} = \sqrt{\frac{\sum_i[(obs_i - calc_i)/\sigma_i]^2}{N_{lines} - N_{const}}}$.
[d] Derived assuming $\alpha_i \approx B_0 - B_i$.
[e] Derived from relative intensity measurements. See text and Figure 5.

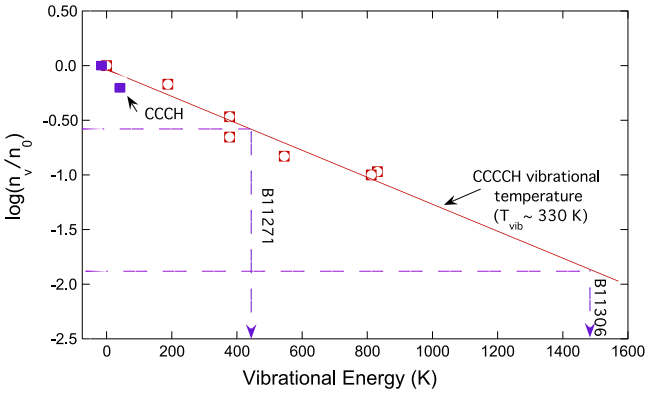

Figure 5. Relative intensity normalized to the ground state vs. excitation energy for the observed states of C_3H (purple solid squares, with ±10% intensity uncertainties approximately corresponding to the size of each box) and C_4H (red open squares; see Cooksy et al. 2015). Vibrational energies for the new $^2\Sigma$ states have been estimated assuming that these states arise from low-lying bending modes and that C_3H radical has the same T_{vib} in our glow discharge source as C_4H.

The hydrogen Fermi-contact parameters (Table 3) appears to support these assignments. This parameter is large and negative for the $B11271$ and $B11222$ states, but nearly zero for the $B11306$ and $v_4 = 1$ $^2\Sigma^\mu$ states. If the bending motion is perpendicular to the p_π orbital of the unpaired electron (i.e., distortion of A'' symmetry), the unpaired electron orbital has a node at the hydrogen nucleus by symmetry, and b_F will be negative owing to spin polarization effects. However, if the bending motion is parallel to the p_π orbital instead (i.e., distortion to A' symmetry), the Fermi contact term should be positive, but this quantity may be offset somewhat by spin

polarization. Perić et al. (2003; see Figure 1) predict that the lower $^2\Sigma$ state of ν_4 has A' symmetry, while that of ν_5 has A'' symmetry, in agreement with the derived b_F values for the two states ($\nu_4 = 1$ $^2\Sigma^u$ and $B11271$, respectively). Although it is tempting to assign $B11222$ to the upper $^2\Sigma$ state of ν_4 (A'' symmetry), and $B11306$ to the upper $^2\Sigma$ state of ν_5 (A' symmetry) using the same argument, owing to their higher energy, the possibility that they instead arise from still other $^2\Sigma$ states cannot be discounted.

A modest number of weak lines in our original survey (Figure 3) remain unassigned. These lines almost certainly arise from still other $^2\Sigma$ states, because they are observed with comparable intensity with Ne buffer gas, are sensitive to the magnetic field, and some have been linked by DR to lines near 44 GHz. Owing to the lower signal-to-noise ratio, however, no definite assignments have been made, but linkages between the dozen or so remaining lines may be feasible if their line intensities could be improved by a factor of 2 or more.

We thank the anonymous referee for extremely helpful comments regarding how the hydrogen Fermi-contact parameters might be used to support the vibrational assignments, H. Gupta, M. Gerin, S. Thorwirth, and H.S.P. Müller for discussions, and B. Rocher for assistance during initial searches for C_3H^+ in our laboratory. The experimental work is supported by NASA grant NNX13AE59G. K.N.C. was supported by a CfA Postdoctoral Fellowship from the Smithsonian Astrophysical Observatory, and B.A.M. is supported by a Janksy Fellowship from NRAO. We also thank E.S. Palmer and P. Antonucci for technical assistance.

REFERENCES

Amano, T. 2010, ApJL, 716, L1
Anicich, V. G., & Huntress, W. T., Jr. 1986, ApJS, 62, 553
Bohme, D. K., Raksit, A. B., & Fox, A. 1983, JAChS, 105, 5481
Botschwina, P. 1991, JChPh, 95, 4360
Botschwina, P., Oswald, R., & Rauhut, G. 2011, PCCP, 13, 7921
Brünken, S., Kluge, L., Stoffels, A., Asvany, O., & Schlemmer, S. 2014, ApJL, 783, L4
Caris, M., Giesen, T. F., Duan, C., et al. 2009, JMoSp, 253, 99
Cernicharo, J., Guélin, M., Agúndez, M., McCarthy, M. C., & Thaddeus, P. 2008, ApJL, 688, L83
Cooksy, A. L., Gottlieb, C. A., Killian, T. C., et al. 2015, ApJS, 216, 30
Cordiner, M. A., Buckle, J. V., Wirström, E. S., Olofsson, A. O. H., & Charnley, S. B. 2013, ApJ, 770, 48
Crabtree, K. N., Martinez, O., Jr., & McCarthy, M. C. 2013, JPCA, 117, 11282
Ding, H., Pino, T., Güthe, F., & Maier, J. P. 2001, JChPh, 115, 6913
Lindemann, E., Rozett, R. W., & Koski, W. S. 1972, JChPh, 57, 803
Fehér, M., & Maier, J. P. 1994, CPL, 227, 371
Fortenberry, R. C., Huang, X., Crawford, T. C., & Lee, T. J. 2013, ApJ, 772, 39
Gottlieb, C. A., Apponi, A. J., McCarthy, M. C., Thaddeus, P., & Linnartz, H. 2000, JChPh, 113, 1910
Gottlieb, C. A., McCarthy, M. C., & Thaddeus, P. 2010, ApJS, 189, 261
Gottlieb, C. A., Vrtilek, J. M., Gottlieb, E. W., Thaddeus, P., & Hjalmarson, Å 1985, ApJL, 294, L55
Graf, S., Geiss, J., & Leutwyler, S. 2001, JChPh, 114, 4542
Gupta, H., Gottlieb, C. A., McCarthy, M. C., & Thaddeus, P. 2009, ApJ, 691, 1494
Huang, X., Fortenberry, R. C., & Lee, T. J. 2013, ApJL, 768, L25
Ikuta, S. 1997, JChPh, 106, 4536
Jäger, W., & Gerry, M. C. L. 1995, JChPh, 102, 3587
Jiang, Q., Rittby, C. M. L., & Graham, W. R. M. 1993, JChPh, 99, 3194
Killian, T. C., Gottlieb, C. A., & Thaddeus, P. 2007, JChPh, 127, 114320
Lattanzi, V., Gottlieb, C. A., Thaddeus, P., Thorwirth, S., & McCarthy, M. C. 2010, ApJ, 720, 1717
Mazzotti, F. J., Raghunandan, R., Esmail, A. M., Tulej, M., & Maier, J. P. 2011, JChPh, 134, 164303
McCarthy, M. C., Chen, W., Travers, M. J., & Thaddeus, P. 2000, ApJS, 129, 611
McCarthy, M. C., & Thaddeus, P. 2005, JChPh, 122, 174308
McCarthy, M. C., & Thaddeus, P. 2008, JChPh, 129, 054314
McCarthy, M. C., Crabtree, K. N., & Martinez, O., Jr. 2013, in 68th Ohio State Univ. Int. Symp. on Molecular Spectroscopy (Columbus, OH: Ohio State Univ.)
McCarthy, M. C., Gottlieb, C. A., Gupta, H., & Thaddeus, P. 2006, ApJL, 652, L141
McGuire, B. A., Carroll, P. B., Gratier, P., et al. 2014a, ApJ, 783, 36
McGuire, B. A., Carroll, P. B., Sanders, J. L., III, et al. 2014b, MNRAS, 442, 2901
Pearson, J. C., Gottlieb, C. A., Woodward, D. R., & Thaddeus, P. 1988, A&A, 189, L13
Perić, M., Mladenović, M., Tomić, K., & Marian, C. M. 2003, JChPh, 118, 4444
Pety, J., Gratier, P., Guzmán, V., et al. 2012, A&A, 548, A68
Radom, L., Hariharan, P. C., Pople, J. A., & v. R. Schleyer, P. 1976, JAChS, 98, 10
Sakai, N., Shiino, T., Hirota, T., Sakai, T., & Yamamoto, S. 2010, ApJL, 718, L49
Sanz, M. E., McCarthy, M. C., & Thaddeus, P. 2005, JChPh, 122, 194319
Savić, I., & Gerlich, D. 1994, in Molecules and Grains in Space, ed. I. Nenner (New York: AIP), 505
Schilke, P., Neufeld, D. A., Müller, H. S. P., et al. 2014, A&A, 566, A29
Sharp-Williams, E. N., Roberts, M. A., & Nesbitt, D. J. 2011, JChPh, 134, 064314
Sumiyoshi, Y., Katsunuma, H., Suma, K., & Endo, Y. 2005, JChPh, 123, 054324
Suzuki, H., Ohishi, M., Kaifu, N., Ishikawa, S.-I., & Kasuga, T. 1986, PASJ, 38, 911
Tanaka, K., Sumiyoshi, Y., Ohshima, Y., Endo, Y., & Kawaguchi, K. 1997, JChPh, 107, 2728
Tenenbaum, E. D., Dodd, J. L., Milam, S. N., Woolf, N. J., & Ziurys, L. M. 2010, ApJS, 190, 348
Thaddeus, P., Gottlieb, C. A., Hjalmarson, Å., et al. 1985, ApJL, 294, L49
Turner, B. E., Herbst, E., & Terzieva, R. 2000, ApJS, 126, 427
Wakelam, V., Smith, I. W. M., Herbst, E., et al. 2010, SSRv, 156, 13
Wang, Y., Braams, B. J., & Bowman, J. M. 2007, JPCA, 111, 4056
Wilson, S., & Green, S. 1980, ApJ, 240, 968
Woon, D. E. 1995, CPL, 244, 45
Woon, D. E., & Herbst, E. 2009, ApJS, 185, 273
Yamamoto, S., Saito, S., Suzuki, H., et al. 1990, ApJ, 348, 363